RSC Advances

ROYAL SOCIETY OF CHEMISTRY

www.rsc.org/advances

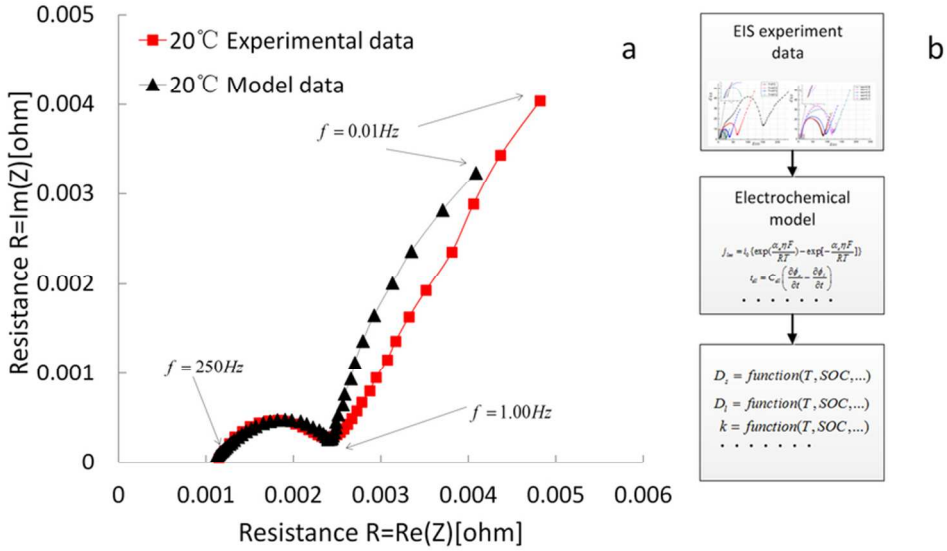

A new electrochemical impedance spectroscopy model and a preliminary parameter identification strategy are proposed in the paper.
40x22mm (600 x 600 DPI)

A new electrochemical impedance spectroscopy model and a preliminary parameter identification strategy are proposed in the paper.

A new electrochemical impedance spectroscopy model of a high-power lithium-ion battery

J.G. Zhu*, Z.C. Sun, X.Z. Wei, H.F. Dai

Clean Energy Automotive Engineering Center, School of Automotive Engineering, Tongji University, Shanghai, 201804, China

*Corresponding author. Tel.: +8618818203849; fax: +8602169589121.

E-mail address: jgzhu@foxmail.com (J.G. Zhu)

Abstract:

This paper presents an electrochemical impedance spectroscopy battery model including the electrical double layer capacitance, which can comprehensively depict the internal state of the battery. Based on the porous electrode theory, the model can obtain a complete spectrum of the cell impendence. And the EIS data recorded by appropriate measurement instrument are of great consistence with the records of theoretical impedance derived from the model in terms of room temperature. To establish the relationship between the internal parameters and external spectrum, a virtual simulation experiment is conducted to illustrate the effect of key parameters on EIS. According to the simulation experiment results, the model can be used to identify internal parameters based on the practical external spectrum. In the last part of the paper, a preliminary parameter identification strategy is proposed to study the relation between battery internal parameter and external conditions.

Key words: Lithium-ion battery; Porous electrode theory; Electrochemical Impedance Spectroscopy model; Parameter identification;

1. Introduction

Due to the long life cycles, good stability, high energy density and voltage platform, the lithium-ion battery among others has been proved to be the ideal power supply not only for the pure electric vehicles (EV) but also for hybrid electric vehicles (HEV) as accessorial energy sources [1,2].

A certain number of previous relative researches on the modeling and experiments of lithium-ion battery have been accomplished. On the aspect of battery characteristic study, the EIS (electrochemical impedance spectroscopy) method, as one of the most accurate methods is applied to model its electrochemical system [3-6], predict battery lifetime [7], estimate the state of charge of battery [3] and obtain the thermal characterization [8,9]. In these studies, the EIS measurements are performed at different frequency ranges using potentiostatic mode with small amplitude signal [10]. In published works, two ways summarized to obtain the battery characteristics from the EIS data. It can be implemented directly for precise analysis [11-13] and parameter identification based on the equivalent circuits [4, 11, 14-17]. Most of lithium-ion battery models today are based on ECM (equivalent circuit models). In the ECM approach, the associated equivalent circuit is used as the tool to predicted battery characteristics. These models are composed of electrical components (resistances, inductances, capacitances, Warburg impedance, constant phase element…) with values identified via EIS.

However, observation and prediction inside battery status by ECM for its rare parameters is difficult. Thus, a mathematical model of higher accuracy for the battery is required. The electrochemical model, including multi-parameters, can reflect the complicated state inside the battery [18-23]. Compared with the equivalent circuit battery model, the electrochemical one, which is based on the porous electrode theory, gains an unprecedented popularity among engineers [21, 24, 25]. Now the electrochemical models are usually intended for simulating the battery behavior during a period of time varying from few minutes to hours. Besides, this electrochemical model is seldom employed for the research on the frequency response,

especially on the EIS study of the battery.

The objective of this paper is to derive a new electrochemical impedance spectroscopy model based on the porous electrode theory, from which a battery complete spectrum can be simulated. The simulation results are in good agreement with experimental ones. And the model is also utilized to obtain the impact of battery inner parameters, such as electrochemical reaction rate constant, diffusion coefficient, conductivity et al, on the simulation impedance spectrum. At last, a preliminary parameter identification strategy, using the EIS model as a linkage, is designed to identify the relations between external conditions and battery inner parameters.

2. Mathematical model

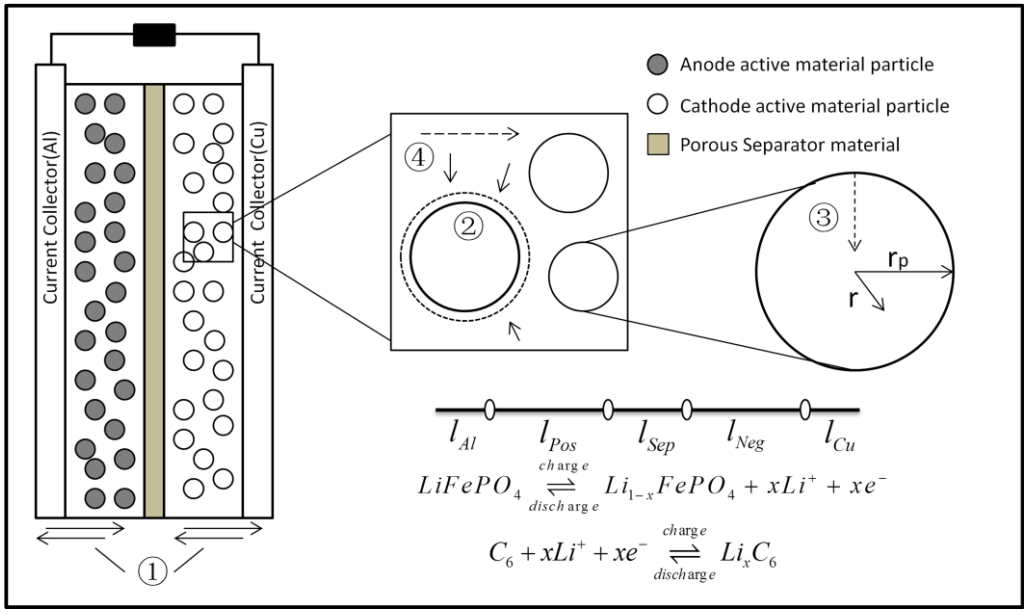

Fig.1 Electrochemical model schematic based on porous electrode theory

The lithium-ion battery includes the ion “insert” and “de-insert” process, a schematic of a lithium-ion battery is shown in Fig.1. It consists of the current collectors, the positive electrode, the separator and the negative electrode. In this model, the lithium-ion battery is taken as a porous mass filled by electrolyte [18]. The basic electrode process in the model is divided into electronic conduction, electrode reaction process, diffusion in solid phase, electrolyte phase lithium-ion transfer and diffusion. Because EIS is a frequency-based analysis method, an electric double layer capacitor mathematical model is added to

improve the veracity of model.

2.1 Electronic conduction

During battery charge and discharge, the electronic conduction process occurs only in the current collector and solid active electrode, as shown in fig.1①. In the model, the ϕ_s and i_s obey the ohm's law.

$$i_s = \sigma_s^{eff} \frac{\partial}{\partial x}\phi_s, \sigma_s^{eff} = \varepsilon_s^{\gamma}\sigma_s \qquad (1)$$

Where ϕ_s is the electrode potential, i_s is the current in solid phase, σ_s^{eff} is the porous electrode equivalent conductivity, σ_s is the conductivity in solid electrode material, ε_s is the porous electrode porosity, γ is the bruggeman porosity exponent.

2.2 Electrode reaction process

The electrode reaction includes the electrochemical charge transfer and the electric double layer reaction.

The model assumes that the electrode reaction occurs at the active surface of the spherical particles in the solid matrix because of the battery electrode porous characteristic as shown in the dashed circles in Fig.1 ②. In the model, The geometry of the solid phase active solid particles is much smaller than the thickness dimension of the electrode.

(1) The electrode reaction current generates at the interfaces of the positive electrode/electrolyte and the electrolyte/negative electrode, which can be calculated from the Butler-Volmer theory [19].

$$j_{loc} = i_0\{\exp(\frac{\alpha_a \eta F}{RT}) - \exp[-\frac{\alpha_c \eta F}{RT}]\} \qquad (2)$$

Where j_{loc} is the transfer current per unit interfacial area, α_a and α_c is anodic and cathodic transfer coefficient, i_0 is exchange current density, η is the over-potential of the intercalation reaction, F is Faraday constant, R is gas constant, T is temperature, i_0 is calculated from the following equation [20].

$$i_0 = Fk_0\sqrt{c_l(c_{s,\max} - c_{s,surf})c_{s,surf}} \qquad (3)$$

Where k_0 is the electrochemical reaction rate constant, c_l is the concentration of lithium ion in

electrolyte, $c_{s,surf}$ is concentration of lithium ion in the reaction interface, $c_{s,\max}$ is theoretical maximum concentration in solid electrode active material.

The over-potential of the intercalation reaction can be obtained in the reference [21]:

$$\eta = \phi_s - \phi_l - E_{eq}(soc) \quad (4)$$

Where ϕ_l is the electrolyte phase potential, $E_{eq}(soc)$ is the open-circuit potential, which is dependent on soc and defined by equation (5), the E_{eq} is approximate based on experimental data. The potential of LiFePO4 vs. Li and the potential of MCMB vs. Li are shown in Fig.2. And the functional relationship is input to the 1-D model as the E_{eq_pos} and E_{eq_neg}.

$$soc = \frac{c_{s,surf}}{c_{s,\max}} \quad (5)$$

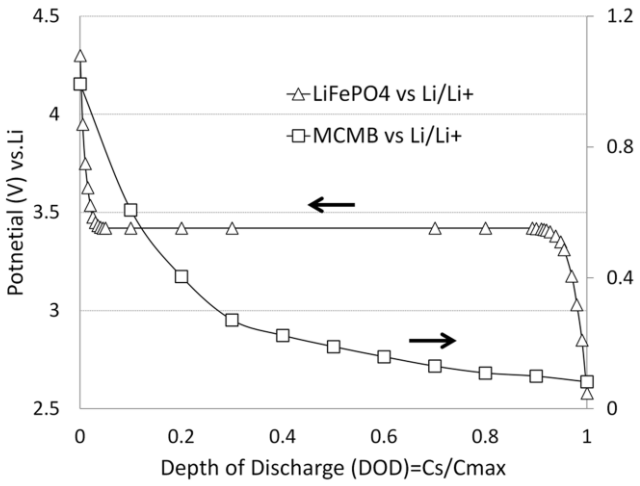

Fig.2 Potential LiFePO4 vs. Li/Li+ and Potential MCMB vs. Li/Li+

(2) Non-faraday current (electric double layer reaction). The current density beside the electric double layer varies with the relative potential alternation on either side of the interface reaction , so a "charge/discharge current" is obtained, which is not directly involved into the electrode reaction. According to the definition of non-faraday current, the impedance characteristics of general electrode system can be obtained:

$$i_{dl} = C_{dl}\left(\frac{\partial \phi_s}{\partial t} - \frac{\partial \phi_l}{\partial t}\right) \quad (6)$$

Where i_{dl} is the non-faraday current, C_{dl} is electric double layer capacitance. The double layer

capacitance is usually not taken into account in the lithium-ion battery mathematical models for its small impact on the simulation results during complete charges and discharges. However, it will play a great role in the frequency domain study.

2.3 Diffusion in solid phase

The electrode active material in this model is assumed to consist of spherical particles with diffusion being the mechanism of transport of the lithium ions into the particle. And the conservation of lithium ions in the solid phase of electrodes is described by Fick's law as shown in Fig.1③:

$$\frac{dc_s}{dt} = D_s \frac{\partial}{\partial r}(\frac{\partial c_s}{\partial r}) \qquad (7)$$

Where c_s is the concentration of lithium ion in solid phase, D_s is diffusion coefficient of lithium ion in solid electrode particles, r is electrode particle radial distance.

At the center of the particle, there is no flux, that is:

$$\text{at} \quad r = 0, -D_s \frac{\partial c_s}{\partial r}\bigg|_{r=0} = 0 \qquad (8)$$

The flux, on the surface of the particle, is equivalent to the consuming/producing rate of lithium ions resulted from the electrochemical reaction occurring at the solid/liquid interface.

$$\text{at} \quad r = r_p, -FD_s \frac{\partial c_s}{\partial r}\bigg|_{r=r_p} = \frac{i_v}{A_v} = j_{loc} \qquad (9)$$

Where r_p is radius of electrode particle, and it is a model constant. i_v is the electrode reaction current, A_v is specific interfacial area.

2.4 Electrolyte phase lithium-ion transfer and diffusion

The lithium ion transfer consists of three ways: electric mobility, diffusion and convection. The convection is ignored and each point of the electrolyte is taken as a micro system in this model as shown in Fig.1④. Based on the assumption that the electrolyte is binary solvent, a material balance of lithium ion in the electrolyte is:

$$\varepsilon_l \frac{\partial c_l}{\partial t} = -\frac{i_v}{F} - \nabla\left(-D_l^{eff}\nabla c_l + \frac{i_l t_+}{F}\right) \qquad (10)$$

In the formula (10), the first term $\frac{i_v}{F}$ is the lithium ion reaction source, and the first term in bracket is caused by the diffusion, and the second term is caused by electric migration of lithium ions, where t_+ is lithium ion transference number, which is a model constant. i_l is the current in the electrolyte, c_l is the lithium ion concentration in electrolyte, D_l^{eff} is the lithium ion equivalent electrolyte phase diffusion coefficient, which is expressed as:

$$D_l^{eff} = \varepsilon_l^{\gamma} D_l \qquad (11)$$

Where D_l is diffusion coefficient of lithium ion in electrolyte, the i_l is subject to the electrolyte phase conductivity and ion mobility, so the following shows a modified equation:

$$i_l = -\delta_l^{eff}\nabla\phi_l + \delta_D^{eff}\nabla(\ln c_l), \delta_l^{eff} = \varepsilon_l^{\gamma}\delta_l \qquad (12)$$

Where δ_l is conductivity of the electrolyte, δ_l^{eff} is lithium ion equivalent electrolyte phase conductivity described by concentrated solution theory [22], δ_D^{eff} is lithium ion equivalent mobility.

$$\delta_D^{eff} = \frac{2RT\delta_l^{eff}}{F}[1+\frac{\partial \ln f}{\partial \ln c_l}][1-t_+] \qquad (13)$$

Where f is the mean molar activity coefficient of the electrolyte.

2.5 Charge conservation

According to the Kirchhoff law, the total number of lithium ion in the cross-section of thickness direction is equal to the battery terminal current incentives. The current flowing through the collector (copper, aluminum) is i_{apply}, flowing through the porous electrodes (anode and cathode active electrode) is i_s, i_l, flowing through the cross-sectional of the separator is $i_l' = i_{apply}$.the solid current $i_s = 0$ in the separator. A current conservation formula as shown:

$$i_s + i_l = i_{apply} \qquad (14)$$

Formula (9) describes the electrode reaction, including the lithium ion transfer process and the e^- conduction process in solid phase, the solid current is divided into faraday current (reaction current) and

non-faraday current (double electric layer reaction), the following formula shows the relation:

$$\nabla i_s = i_v + i_{dl} \qquad (15)$$

3. Result and discussion

3.1 Model verification

The battery adopts in experiments is a Suzhou Phylion commercial lithium-ion battery, with a nominal capacity of 8Ah. Discharge curves are obtained by the MACCOR 4300 (USA) measurement. The impedance spectrum has been obtained using an electrochemical workstation (MACCOR FRA-0356, USA) driven by a computer. The temperature is controlled and monitored by an ESPEC environmental chamber. The solution of the model is performed by using the geometric multi-grid iterative type solver on the platform of the commercial software COMSOL MULTIPHYSICS ® (Version 4.2a) and MATAB 2011b.

In order to test the validity of the model, a comparative analysis of experiment and simulation are implemented. Discharge experiments are carried out at room temperature (20℃). Fig.3 illustrates the calculated discharge curves derived from the model and experimental data. As discharge rate varies from 0.5 to 2C, the experimental discharge curves effectively validate the modeling results. The parameters used in the model are listed in the table 1.

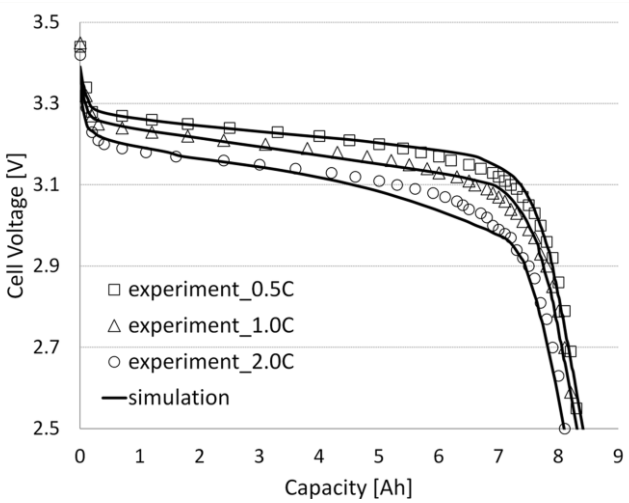

Fig.3 Simulation and experimental constant-current discharge curves at 20℃

The triangle line in Fig.4 represents the simulation results of EIS obtained through the mathematical

model described above, while the black square one shows the experiment data. They are potentiostatically measured with an AC oscillation of 5mV amplitude voltage, and the frequencies are ranging from 10 KHz to 0.01Hz. The tests are performed at 50% SOC but 20℃ and 30℃respectively.

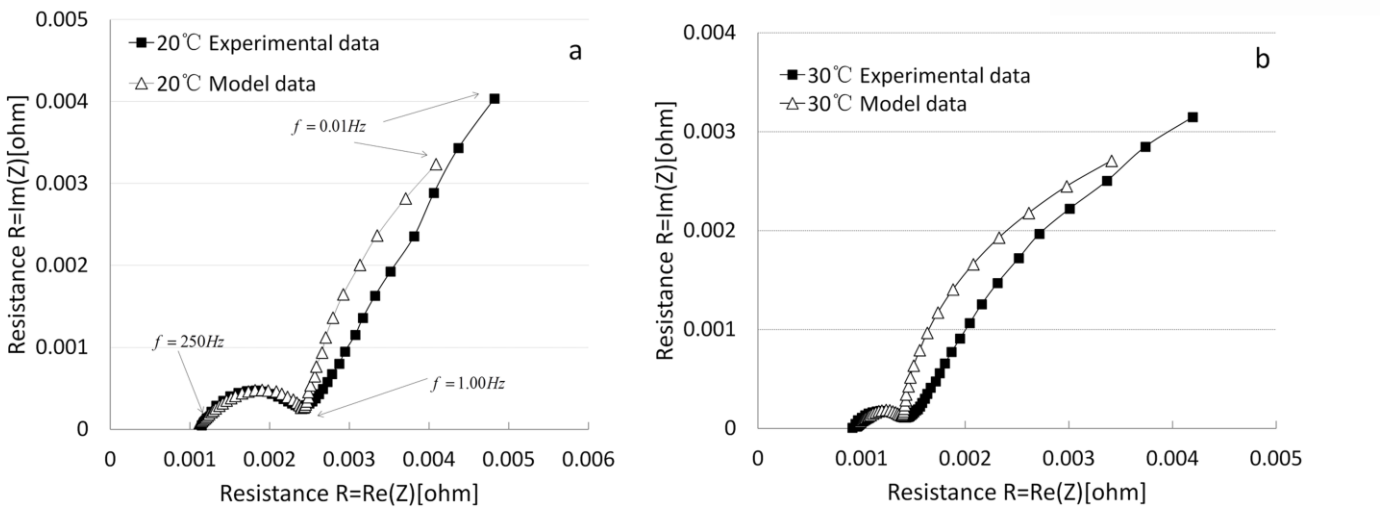

Fig.4 the impedance spectra of the battery from the experimental data and the model simulation; Fig.4a EIS at 50% SOC and 20℃；Fig.4b EIS at 50% SOC and 30℃

The shape of the simulated semi-circle quite fit the measured one in the Fig.4. To make further discussion, the impedance spectra can be divided into two sections: the mid-frequency section and the low-frequency one.

In the low-frequency section (1.00Hz~0.01Hz), the curve experiences a steady increase of impedance, which stands for the lithium-ion diffusion process [12, 24]. Some researchers assert that the process represents the lithium ion diffusion in the solid phase while others argue it as a combined action of solid and electrolyte phase diffusion. The study in this paper shows that the previous part of the low-frequency section in EIS is affected by electrolyte phase diffusion coefficient. J.Jin et al [11] shows, in his paper, the Nyquist Diagrams of the EIS measurements for Li/LiFePO4 cells incorporating two kinds of electrolytes and the low-frequency section witnesses a sharp change in the line slope. This further proved our point of view, and we will discuss it later in the 3.2 chapter.

The mid-frequency section (300Hz~1.00Hz) forms a depressed semicircle, which is a well-known

phenomenon in the electrochemistry [6]. It represents the electrochemical reaction, including the charge transfer and double layer reaction.

In Fig.4, the curve of the simulated semi-circle achieves a superb fitting effect in the mid-frequency area, while the accomplishment of the counterpart in the low frequency section is relatively poor. The work is still in progress, so a doubtless explanation for the slope observed at lower frequencies cannot be provided. There might some inadequate factor in our model or some parameter values, which still need to be investigated.

The Bode plot at 20℃, as shown in Fig.5 can also be used to fit the experimental data as the same way that the impedance spectrum was used.

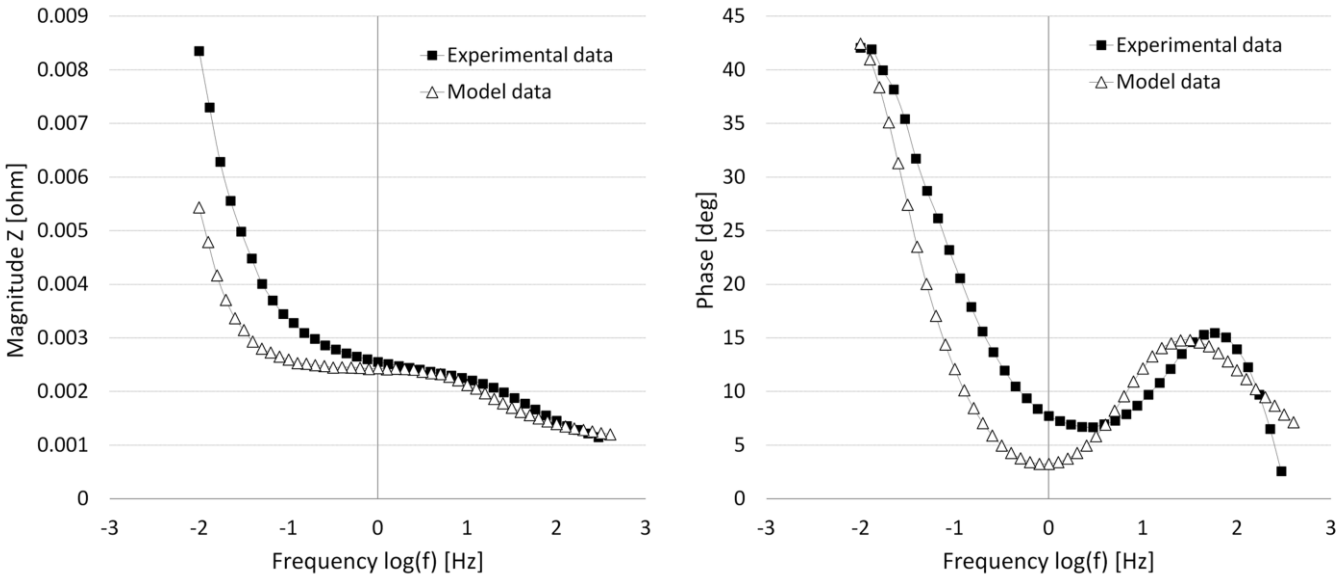

Fig.5 Bode plot of the battery impedance from the experimental data and the model simulation at 50% SOC and 20℃

Parameters used in this model are established based on the solid foundation of experimental measurements, references and estimation. Necessary parameters of an 8Ah LiFeO4 battery model are showed in Table 1.

Table 1 Model Parameters at 50% SOC and 20℃

Model parameter	Value	Description

r_{p_neg}	2.5e-6(m) [b]	Particle radius Negative
r_{p_pos}	5.2e-8(m) [b]	Particle radius Positive
k_{0_neg}	2e-11(m s^{-1}) [18, 21]	electrochemical reaction rate constant negative
	4e-11(m s^{-1}) [a] (30℃)	
k_{0_pos}	2e-11(m s^{-1}) [18, 21]	electrochemical reaction rate constant positive
	4e-11(m s^{-1}) [a] (30℃)	
D_{s_neg}	9e-14(m^2 s^{-1}) [23]	Solid phase lithium diffusion coefficient Negative
D_{s_pos}	8e-18(m^2 s^{-1}) [18]	Solid phase lithium diffusion coefficient Positive
$c_{s\_neg,\max}$	26390(mol m^{-3}) [18,21]	Maximum solid phase lithium concentration Negative
$c_{s\_pos,\max}$	22800(mol m^{-3}) [18,21]	Maximum solid phase lithium concentration Positive
c_0	2000(mol m^{-3}) [26]	Initial electrolyte salt concentration
c_{s0_pos}	11400(mol m^{-3}) [b]	Initial Positive State of Charge
c_{s0_neg}	14863(mol m^{-3}) [b]	Initial Negative State of Charge
D_l	3e-11(m^2 s^{-1}) [a]	Electrolyte phase lithium-ion diffusion coefficient
	4.5e-11(m^2 s^{-1}) [a] (30℃)	
α_{a,c_pos}	0.5[a]	transfer coefficients of electrode reactions positive
α_{a,c_pos}	0.5[a]	transfer coefficients of electrode reactions negative
γ	1.5[a]	Bruggeman porosity exponent
ε_{s_pos}	0.38[b]	Solid phase volume fraction Positive
ε_{s_neg}	0.65[b]	Solid phase volume fraction Negative
ε_{l_pos}	0.41[b]	Electrolyte phase volume fraction Positive
ε_{l_neg}	0.15[b]	Electrolyte phase volume fraction Negative
σ_{s_pos}	0.005(s m^{-1}) [18]	Conductivity of positive
σ_{s_neg}	100(s m^{-1}) [23]	Conductivity of negative

l_{Neg}	40e-6(m) [b]	The length of negative
l_{Sep}	40e-6(m) [b]	The length of separator
l_{Pos}	35e-6(m) [b]	The length of positive
l_{Al}	1e-5(m) [b]	The length of positive collector
l_{Cu}	1.5e-5(m) [b]	The length of negative collector
C_{dl}	4 (F m^{-2}) [a]	Electric double layer capacitance
	5 (F m^{-2}) [a] (30℃)	
δ_l	δ_l [19]	electrolyte phase conductivity
	1.6 δ_l [a]	
T	293(K)	temperature
R	8.3145 (J mol^{-1} K^{-1})	gas constant
F	96487(C mol^{-1})	Faraday's constant
t_+	0.363[26]	Lithium-ion transference number

[a] Estimated

[b] Calculated from the practical material and structure of battery

Though these parameters in the model achieve an excellent fitting affection, some adjustments of parameter still need to be modified to fulfill a better fitting effect for other type of cells. It should be pointed out that the electrolyte phase lithium-ion diffusion coefficient is the function of temperature [26], as the battery temperature and concentration alternates slightly in the EIS test, in order to simplify the mathematical model and the study of the parameters impact on the EIS, an estimation of the correction parameters was accomplished on the basis of reference in the simulation in the mathematical model [19].

3.2 The effect of key parameters on EIS

The model based on multiple parameters of porous electrode theory is capable of reflecting the internal characteristics of the battery. Being subjected to outside influence, the alternations of impedance spectroscopy generally are the results rendered by the combination of several factors. So it is difficult to identify the inside status of the battery simply by external characteristic impedance spectroscopy. The first

priority is given to study the relationship between the key parameters and the spectra inside the battery to find the impact of the variation of the impedance spectra, which provide the basis for the identification of the battery status and spectra based reference.

Related to the battery, some parameters are invariable, such as the physical size, the Faraday's constant et al, that are independent of external conditions, while other parameters are usually influenced by the environment. In this paper four key parameters are thoroughly adopted, which are electrochemical reaction rate constant, electrolyte ionic conductivity, solid phase lithium-ion diffusion coefficient and electrolyte phase lithium-ion diffusion coefficient. Then, a proportional coefficient k was defined to modify the parameter values. The characteristics of EIS with different parameters are obtained by simulation.

$$\text{New Parameter value} = k \times \text{Parameter value}$$

Fig.6 shows the results when different solid phase lithium-ion diffusion coefficient parameters are involved. The effect of electrolyte ionic conductivity on EIS is shown in Fig.7. As shown in Fig.8, a dramatic effect of the variation of electrolyte phase lithium-ion diffusion coefficient on the model is observed. Fig.9 shows the effect of electrochemical reaction rate constant on the EIS. The impedance spectra are simulated at 50% SOC with frequencies ranging from 100 KHz to 0.01Hz at room temperature.

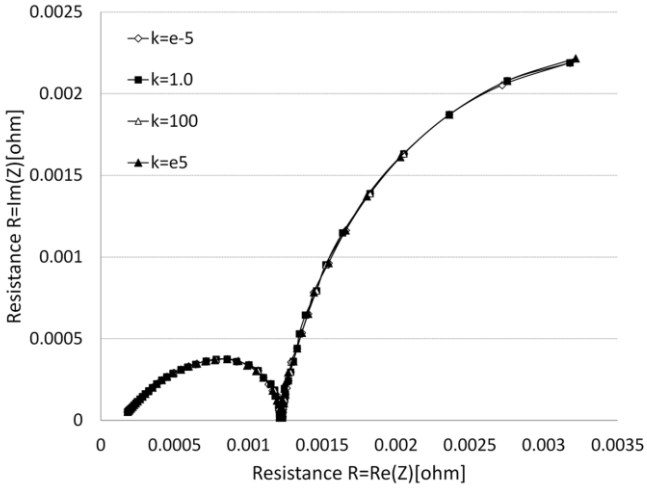

Fig.6 Variation of impendence spectrum at various solid phase lithium-ion diffusion coefficient in simulation

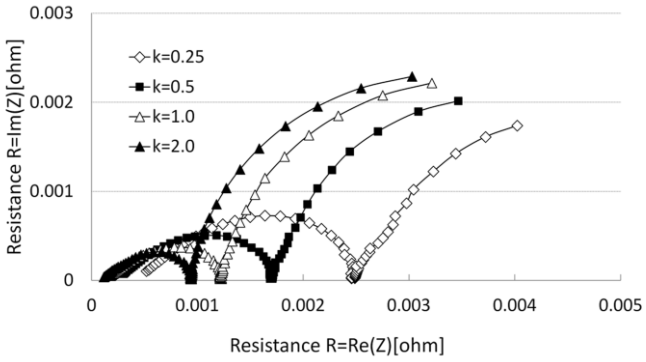

Fig.7 Variation of impendence spectrum at various electrolyte phase ionic conductivity in simulation

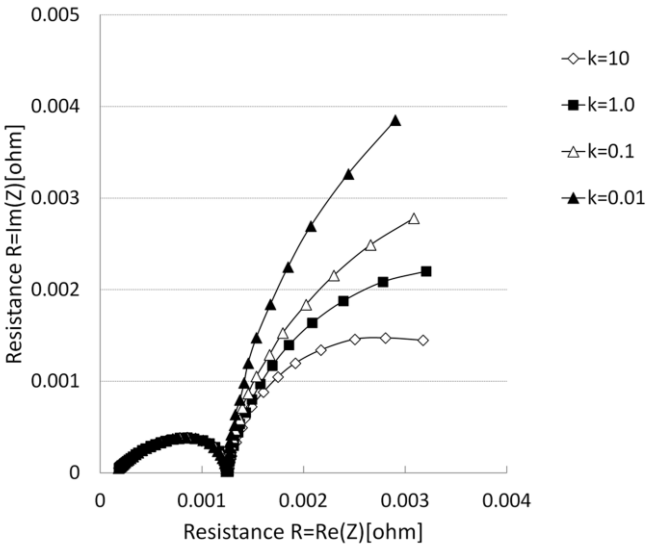

Fig.8 Variation of impendence spectrum at various electrolyte phase lithium-ion diffusion coefficient in simulation

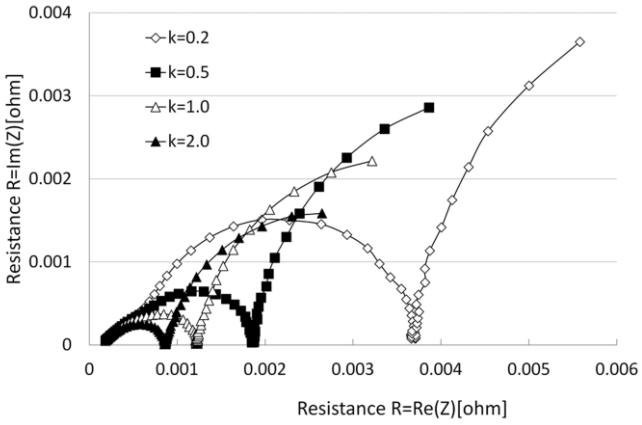

Fig.9 Variation of impendence spectrum at various electrochemical reaction rate constant in simulation

3.2.1 Discussion on effect of lithium-ion diffusion coefficient in solid phase

Usually, the solid phase lithium-ion diffusion coefficient mainly affects the low-frequency process. However, according to Fig.6, with significant changes of the lithium ion diffusion coefficient, the impedance characteristics of the model only experience some slight fluctuations. The impedance of the solid phase

diffusion is mainly embodied in the formula (7). And thus the conclusion shows that the internal concentration gradient in the solid phase particles has a negative relation with the diffusion resistance. The emerging of constant low-frequency resistance in the simulation was due to the following causes: Firstly, the shortage of the incentive time in our model. Fig.10 and Fig.11 show the center and surface concentration of the solid particles, and the incentive frequency are 0.1Hz and 0.01Hz respectively. The x-axis represents the 1-D model from left to right as Cu collector, negative, separator, positive, Al collector. The y-axis represents the concentration values. The lithium ion concentration in the center of the particles has no enough time to reaction due to the shortage of time, but the surface concentration varies evidently, so the obvious observation of the concentration gradient variation would not be observed. Besides, according to the formula (8) (9), the effect of resistance on the impedance spectrum is relatively less significant. Fig.12 shows the changes of electrolyte salt concentration under the AC excitation at various solid phase lithium-ion diffusion coefficient. X-axis represents the 1-D model which is the same as Fig.10 and Fig.11. Y-axis represents the concentration of the value deviation from the initial value. To analyze the impact of solid phase diffusion coefficient on the internal reaction process, the concentration distribution at various electrolyte phase lithium-ion diffusion coefficient is shown in Fig.13. From Fig.12 and Fig.13, the distribution of electrolyte salt concentration is affected by the excitation frequency obviously. The smaller the excitation frequency is the more uneven concentration distribution is. However, the changing of the diffusion coefficient of the solid phase has seldom effect on the concentration distribution. Combined with Fig.10 and Fig.11, the conclusion could be drawn that the solid phase diffusion of lithium ion does not occur, and even if it happens but produces little affection under 0.01Hz. Therefore, significant changes of the solid phase lithium-ion diffusion coefficient only experience some slight fluctuations in our model. There might be a missing phenomenon somewhere in our model or some parameter values still to be investigated.

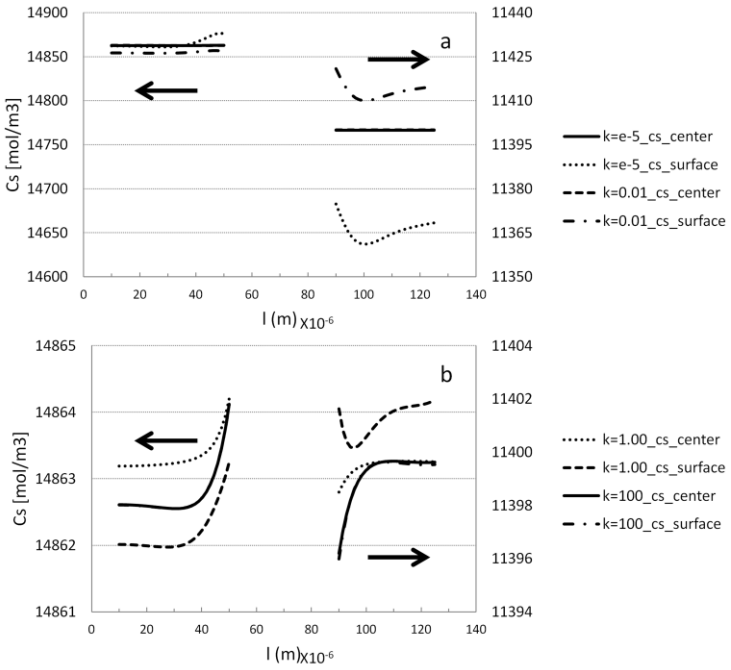

Fig.10 the center and surface lithium ion concentration of the particle under 0.1Hz: The x-axis represents the 1-D model from left to right as Cu collector, negative, separator, positive, Al collector; The y-axis represents the concentration values

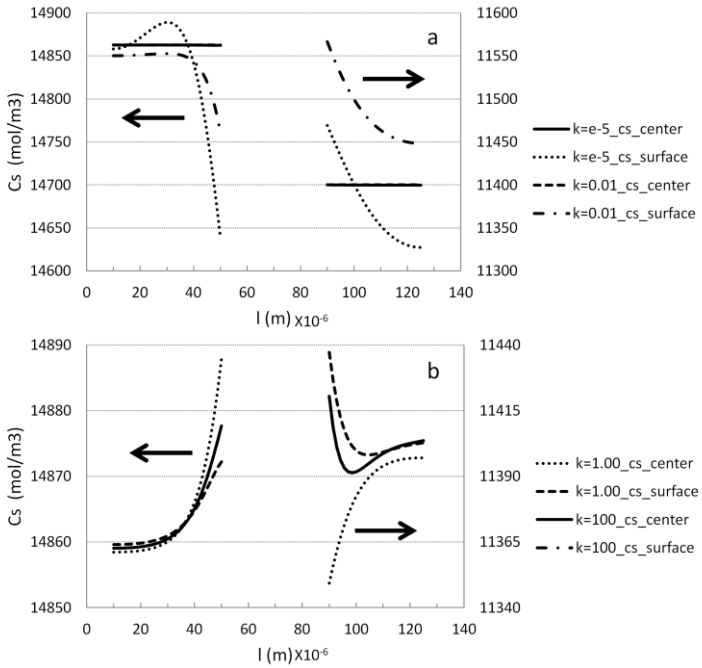

Fig.11 the center and surface lithium ion concentration of the particle under 0.01Hz: The x-axis represents the 1-D model from left to right as Cu collector, negative, separator, positive, Al collector; The y-axis represents the concentration values

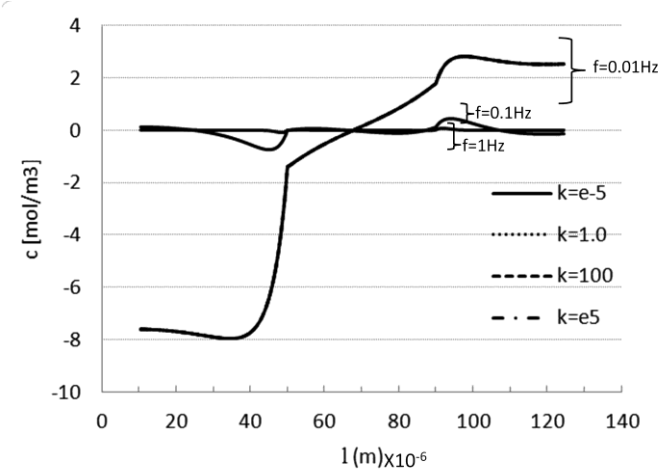

Fig.12 Variation of electrolyte salt concentration at various solid phase lithium-ion diffusion coefficient: The x-axis represents the 1-D model from left to right as Cu collector, negative, separator, positive, Al collector; Y-axis represents the concentration of the value deviation from the initial value

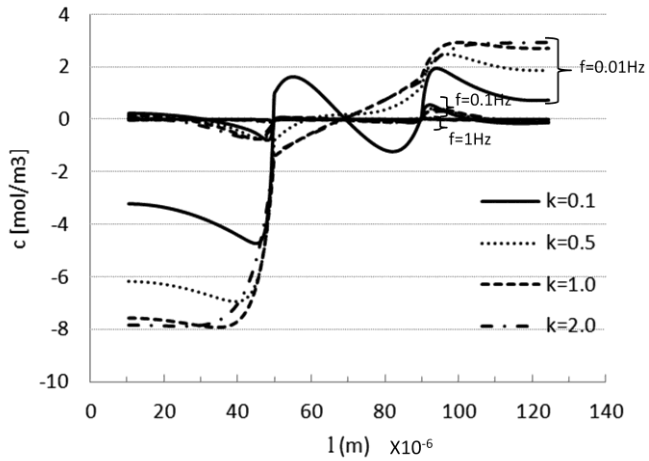

Fig.13 Variation of electrolyte salt concentration at various electrolyte phase lithium-ion diffusion coefficient: The x-axis represents the 1-D model from left to right as Cu collector, negative, separator, positive, Al collector; Y-axis represents the concentration of the value deviation from the initial value

3.2.2 Discussion on effect of electrolyte ionic conductivity

The battery ohm resistance is positively associated with the electrolyte ionic conductivity, and the resistance decreases with the parameter increasing. The picture Fig.7 shows the performance that the intersection of the spectrum and the horizontal axis offset to the left. The reaction of Lithium-ion battery, based on the porous electrode theory, is an actually “insert” and “de-insert” process, which can be further divided into electronic transfer, Lithium-ion diffusion in electrolyte, electrode reaction and Lithium-ion diffusion in solid phase. Improving the ionic conductivity of lithium ion is to accelerate the ionic transport

and reduce the ohm resistance. The concentration difference of the reaction interface increases due to the almost same solid phase diffusion, thereby affecting the exchange current density and accelerating the reaction rate. The performance is that the electrochemical semi-circle becomes smaller as shown in the Fig.7. So the electrochemical reaction is also associated with electrolyte ionic conductivity.

3.2.3 Discussion on effect of lithium-ion diffusion coefficient in electrolyte

As shown in Fig.8, the amplitude of the low-frequency impedance spectrum is almost affected by electrolyte phase lithium-ion diffusion coefficient. The resistance shows a consistent variation trend with the coefficient. Electrolyte phase lithium-ion diffusion coefficient is independent of the electrochemical reaction process. This phenomenon mainly results from the larger time constant of the diffusion process. Therefore, the electrolyte phase lithium-ion diffusion coefficient mainly affects the low-frequency part in the frequency domain. However, numerous present studies insist that the diffusion is faster in the electrolyte than in the solid and thus the diffusion step in the process is ignored, which is in disagreement with our conclusion. Our study shows that the previous part of the low-frequency section in EIS is affected by electrolyte phase diffusivity.

3.2.4 Discussion on effect of electrochemical reaction rate constant

From Fig.9, the following conclusions can be drawn. The reaction rate primarily influences the mid-frequency process in the spectrum. It has a negative correlation with the impedance of the electrochemical process, the value of the reaction rate decreases while the electrochemical circle increases. The conclusion is consistent with the one adopting the ECM. Reaction rate does not affect the real axis intersection of constant.

According to Arrhenius law, the electrochemical reaction rate constants depend on the temperature, which can be written as: $k' = A_o e^{-E_a/RT}$. Where, A_o is a constant and E_a is the activation energy. Based on the relationship above, it is evident that k' is negatively dependent on temperature, and it indeed

corresponds with the conclusion of our simulation. As shown in Fig.14, the significant effect of the temperature on the region of the mid-frequency on the impedance spectrum may result from the temperature effect on the reaction rate constant.

3.3 Parameter identification strategy

Many studies have shown that the EIS characteristics of battery were obviously influenced by the external environment and internal conditions, especially the temperature and battery charge state. So a series EIS test of the battery at different temperature and under different SOC is conducted. As shown in Fig.14, the ohm resistance decreases gradually with the increase of temperature. However, the charge-transfer reaction occurring at the electrode/electrolyte interface is significantly influenced by the decrease of temperature, and the increase of the temperature exerts obviously impact on the decreases of the charge-transfer resistance. Furthermore, as the operation temperature falls below 10℃ the impedance undergoes a sharp rise. According to the Fig.15, the SOC mainly influences the low-frequency process and the growth of imaginary part of impedance become more evident with the increased SOC. Also there exist almost no appreciable impedance variation in the battery data be observed at intermediate SOC value range, 0.1<SOC<0.9.

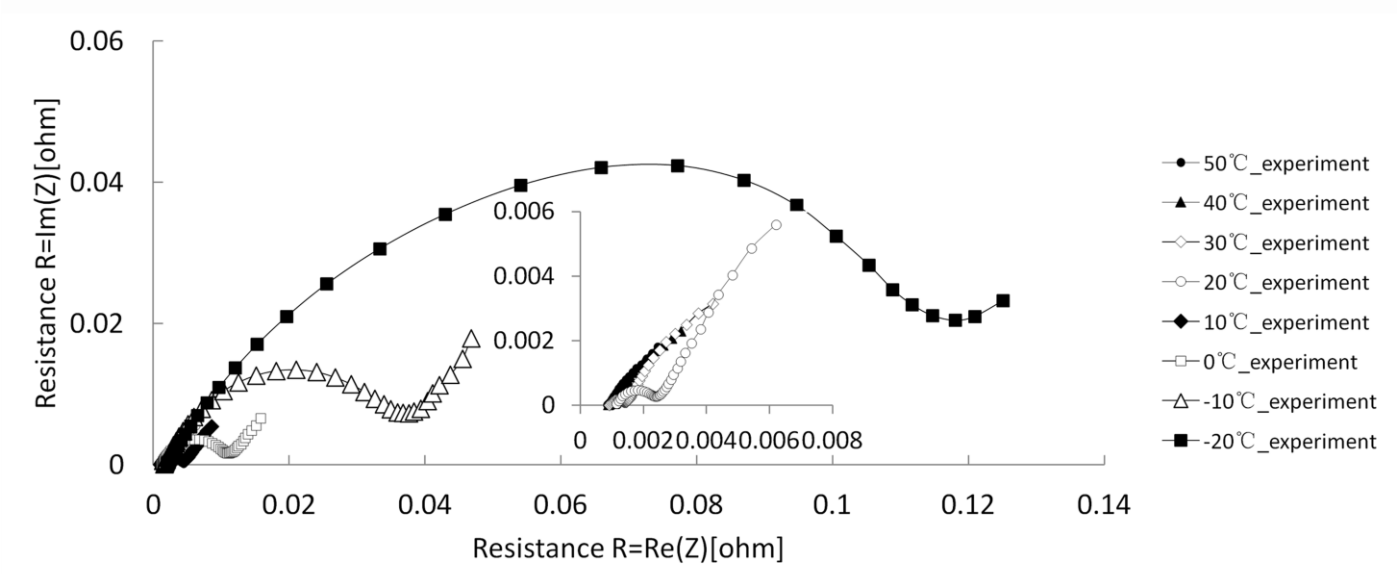

Fig.14 the EIS at various temperature at 50% SOC, frequency range from 10 KHz to 0.01Hz

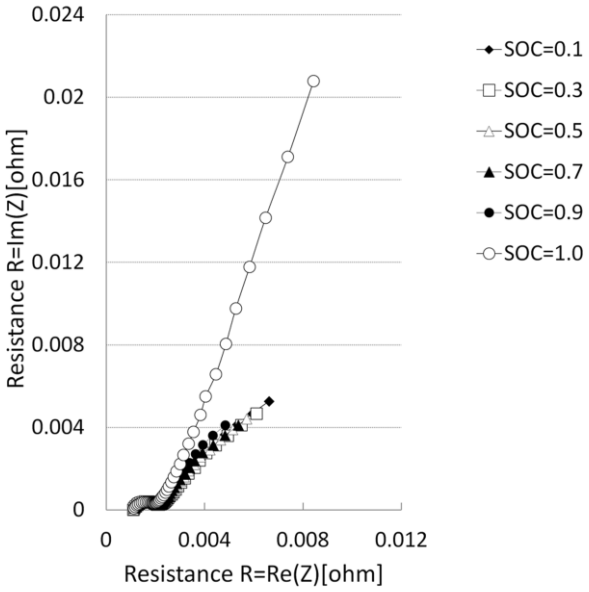

Fig.15 the EIS at various SOC and 20℃, frequency range from 10 KHz to 0.01Hz

Most of studies on the EIS today are based on ECM, the parameter identification strategy is shown in Fig.16a. In the ECM approach, the associated equivalent circuit affords us with easier access to the prediction of battery behavior. However, the ECM encounters two problems. On one hand, it is hard to establish the relation between the ECM parameters and the internal status of battery. On the other hand, a low complexity ECM is inadequate for interpretation and prediction of the physicochemical process. The electrochemical model in this paper involved a multitude of related parameters can thus interpret the dynamics of the battery more sufficiently, which means a thorough analysis of the EIS, as shown in Fig.16b. The relationship between some internal parameters and external spectrum are established by the simulation before. Work is underway to explore the internal parameters accordance with temperature and SOC based the electrochemical model parameter identification strategy .

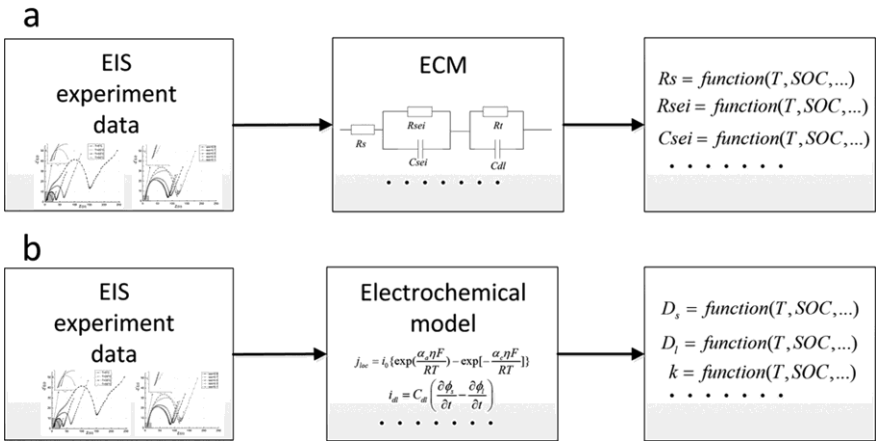

Fig.16 the battery parameter identification strategy; Fig.16a the ECM strategy; Fig.16b the electrochemical model strategy

4. Conclusion

In this paper, an EIS model including electrical double layer capacitance is established to study the impedance characteristics. Firstly, the model results are validated on aspects of discharge curves, which show a high degree of consistency between the modeling results and experimental results. Secondly, the model based on the porous electrode theory can obtain a complete spectrum of the cell impendence. In the mid-frequency range, the model-based simulation results are highly in accordance with the experimental ones at room temperature. Thirdly, the inner physical parameters of battery with the EIS model are identified. Instead of the time-consuming and complicated process, it can gain more information than the ECM. Further research is conducted to explore the effect of internal parameters on the battery by this model. According to the external spectrum, the internal parameters can be effectively identified and predicted by simulating the effect of key parameters on EIS. Apparently, affected by reaction rate and electrolyte ionic conductivity, the change of electrochemical semi-circle is dramatic. Furthermore, our research illustrates that the previous part of the low-frequency is relevant to the electrolyte phase lithium-ion diffusion coefficient. In 0.01Hz and higher frequency range, solid phase diffusion process is not clearly reflected in the impedance spectrum, and the phenomenon is explained in the paper from the aspect of electrode inside process, The electrolyte phase and solid phase diffusion process should have obvious boundaries, and the time constant of the phase

diffusion process in electrolyte is smaller. In-depth research on this phenomenon will be continued in this future work. Based on this model, a new parameter identification strategy is proposed to study the law of battery parameters affected by the environment, and this paper can provide certain referencing value in establishing an accurate battery model and battery design.

Reference

[1] Takahashi M, Tobishima S, Takei K, Sakurai Y, Journal of Power Sources 97-98(2001) 508.

[2] Franco A A. RSC Advances, 2013, 3(32): 13027.

[3] P. Mauracher, E. Karden, Journal of Power Sources 67(1997) 69.

[4] Edward P. Randviir, Craig E. Banks, Anal. Methods, 2013, 5, 1098.

[5] J. Xu, C.Chris Mi, B.Cao, J.Cao, Journal of Power Sources 233 (2013) 227.

[6] J.R. McDonald, Impedance Spectroscopy: Emphasizing Solid Materials and Systems, Wiley-Interscience, 1987.

[7] M. Ecker, J. B. Gerschler, J. Vogel et al. Journal of Power Sources 215 (2012) 248.

[8] J.P.Schmidt, D. Manka, D. Klotz et al. Journal of Power Sources 196 (2011) 8140.

[9] M. Flekenstein, S. Fischer, O. Bohlen et al. Journal of Power Sources 223 (2013) 259.

[10] E. Karden, S. Buller, R.W. De Doncker, Journal of Power Sources 85 (2000) 72.

[11] J. Jin, H.H. Li, J.P. Wei, X.K. Bian, Z. Zhou, J. Yan, Electrochemistry Communications 11(2009) 1500.

[12] F. Varsano, F. Decker, E. Masetti, F. Croce, Electrochimica Acta 46 (2001) 2069.

[13] I. Jimenez Gordon, S. Grugeon, A. Debart et al. Solid State Ionics 237 (2013) 50.

[14] S.S. Zhang, K. Xu, T.R. Jow, Electrochimica Acta 51 (2006) 1636.

[15] X.-Z. Liao, Z.F. Ma, Q. Gong, Y.-S. He, L. Pei, L.-J. Zeng, Electrochemical Communications 10 (2008) 691.

[16] J. Gomez, R. Nelson, E.E. Kalu, M.H. Weatherspoon, J.P. Zheng, Journal of Power Sources 196 (2011) 4826.

[17] M. Ueda, M. Ohe, J.-H. Kim, S. Yonezawa, M. Takashima, Journal of Fluorine Chemistry 149 (2013) 88.

[18] V. Srinivasan, J. Newman, J. Electrochem. Soc, 151 (10) (2004) A1517.

[19] M. Doyle, J. Newman, J. Electrochem. Soc, 143 (1996) 1890-1903.

[20] Doyle M, Newman J, Gozdz A S, et al. Journal of the Electrochemical Society, 1996, 143(6): 1890.

[21] L.Cai, R.E.White, Journal of Power Sources 196 (2011) 5985.

[22] M. Doyle, T. F. Fuller, J. Newman, J. Electrochem. Soc, 140 (1993) 1526.

[23] L. Song, J.W. Evans, J. Electrochem. Soc. 147 (6) 2086-2095 (2000).

[24] S.M. Zhang, J.X. Zhang, S.J. Xu, X.J. Yuan, B.C. He, Electrochimica Acta 88 (2013) 287.

[25] G.-H. Kim, K. Smith, K.-J. Lee, S. Santhanagopalan, A. Pesaran, J. Electrochem. Soc. 158 (8) A995-A969 (2011).

[26] N. Lars Ole Valoen, J. Electrochem. Soc, 152 (2005) A882.